

## **Supporting Information**

### **Mechanical Reinforcement of Free-standing Polymeric Nanomembranes via Aluminosilicate Nanotube Scaffolding**

Anteneh Mersha<sup>1,2</sup> and Shigenori Fujikawa<sup>\*1,2,3,4</sup>

<sup>1</sup> Graduate School of Engineering, Kyushu University, Fukuoka 819-0395, Japan

<sup>2</sup> WPI International Institute for Carbon-Neutral Energy Research (WPI-I2CNER), Kyushu University, Fukuoka 819-0395, Japan

<sup>3</sup> Center for Molecular Systems (CMS), Kyushu University, Fukuoka 819-0395, Japan

<sup>4</sup> Laboratory for Chemistry and Life Science, Tokyo Institute of Technology, 4259 Nagatsutacho, Midori-ku, Yokohama, 226-8503, Japan

#### **Corresponding Author**

\*Email: [fujikawa.shigenori.137@m.kyushu-u.ac.jp](mailto:fujikawa.shigenori.137@m.kyushu-u.ac.jp)

## Experimental

### 1. Materials

Glass substrate was used for thin-film deposition. Poly(4-vinylphenol) (PVP, Mw = 11000, Sigma-Aldrich) was used as sacrificial layer. Tetraethyl orthosilicate (TEOS, Kanto Chemical) and  $\text{AlCl}_3 \cdot 6\text{H}_2\text{O}$  (Wako Ltd.) were used as reactants for aluminosilicate nanotubes (ASNTs) synthesis. Titanium n-butoxide (TBO, Gelest Inc.) was used as  $\text{TiO}_2$  precursor. Polydimethylsiloxane (PDMS, Sylgard® 184) was used to prepare a polymer coating. Ethanol (anhydrous, EMSURE, Germany), chloroform and n-hexane (Wako Ltd.) were used as received. All the chemicals were of analytical grade. Deionized water ( $18.3 \text{ M}\Omega \text{ cm}^{-1}$ , Millipore, Direct-QTM) was used for substrate cleansing and solution preparation.

### 2. Synthesis of ASNTs

ASNTs were synthesized based on previously reported method.<sup>1</sup> It involves simple and inexpensive hydrothermal condensation of dilute concentrations of tetraethyl orthosilicate (TEOS, Kanto Chemical) and  $\text{AlCl}_3 \cdot 6\text{H}_2\text{O}$  (Wako Ltd.) at  $95^\circ\text{C}$  for 96 hours. The surface morphology and Al/Si ratio of the nanotubes were studied by transmission electron microscopy (TEM, JEM 2010) and scanning electron microscope- electron diffraction spectroscopy (SEM-EDS, JSM-7900F) respectively (Figure S1).

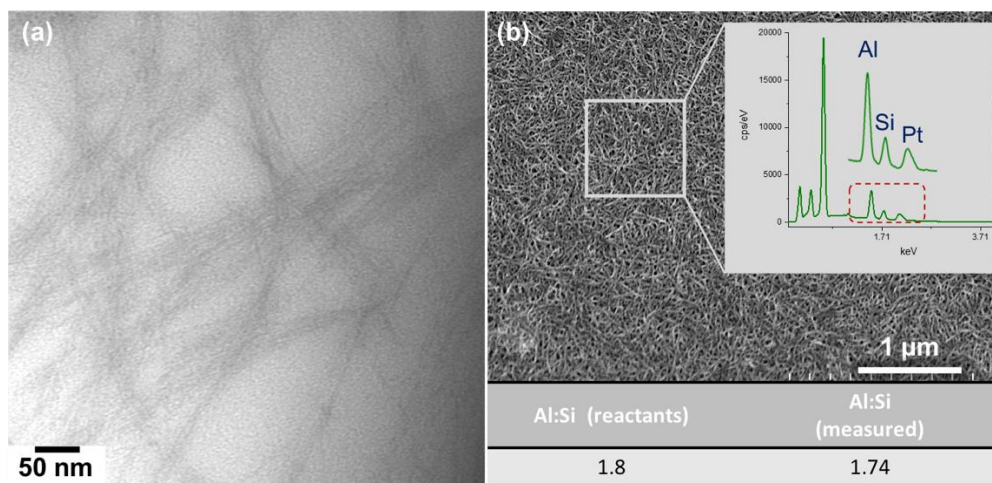


**Figure S1.** (a) TEM micrograph of synthesized ASNT bundles; (b) Ratio of Al to Si in the ASNT product determined by scanning electron microscope-electron diffraction spectroscopy (SEM-EDS). Comparable result has been obtained.

### 3. Nanomembrane preparation procedure

The overall nanomembrane preparation process is illustrated in Figure 1a. Firstly, a cleaned glass substrate was treated by oxygen plasma etching to hydrophilize its surface. Details of the oxygen plasma treatment are outlined elsewhere<sup>2</sup>. A sacrificial polymer substrate of PVP was then spin-coated (3000 rpm, 60 s) from 15 wt% ethanol SOLUTION and annealed at 120°C for 5 minutes.

Subsequently, an as-synthesized aqueous dispersion of ASNTs (0.2–0.3 mg/ml) was deposited on the PVP substrate by carefully optimized spin coating condition. Spinning speed was ramped up from 500 rpm (held for 10 s) to 1500 rpm (for 30 s) and finally to 3000 rpm (for 30 s). The deposited ASNT network was allowed to dry in ambient air for 15 minutes.

Following that, an ultra-dilute solution (1 mM in chloroform) of  $\text{Ti}(\text{O}^n\text{Bu})_4$  was spin-coated (3000 rpm, 60 s). The alternate coating of ASNTs and  $\text{TiO}_2$  was repeated until the desired cycle. Finally, a 1.3 Wt% hexane solution of polydimethylsiloxane (PDMS) was spin-coated at a speed of 4000 rpm for 180 s, and crosslinked at 80°C for 12 hours. The PDMS solution was prepared from Sylgard® 184 kit by mixing 10 parts of the pre-polymer base (part A) and 1 part of the curing agent (part B) as per the manufacturer's instruction.<sup>3</sup> FS-NMs of various thicknesses could be prepared from different PDMS concentrations ranged from 1.3 wt% to 0.6 wt%. The concentration of PDMS was chosen aiming to prepare nanomembranes down to sub-100 nm thicknesses while ensuring their mechanical robustness.

The resulting composite film on the glass substrate was then immersed in ethanol to dissolve the PVP sacrificial layer and release the nanomembrane. Free-standing nanomembranes (FS-NMs) of the general designation  $(\text{A-T})_n/\text{PDMS}$  (where A = ASNTs, T =  $\text{TiO}_2$ , PDMS = polydimethylsiloxane, n = number of cycles of alternate ASNTs and  $\text{TiO}_2$  coating) were fabricated. A similar procedure was followed to prepare  $\text{A}_n/\text{PDMS}$  and  $\text{T}_n/\text{PDMS}$ , except that  $\text{TiO}_2$  was absent in the case of  $\text{A}_n/\text{PDMS}$  and ASNT was absent in the case of  $\text{T}_n/\text{PDMS}$ .

### 4. Characterization

The morphological change during the spin-coating process was examined by field emission scanning electron microscope (FE-SEM, Hitachi S-5200).

To evaluate the penetration of PDMS into the ASNT network structure, elemental analysis on the scaffold-side of the detached (A-T)<sub>10</sub>/PDMS membrane was conducted by X-ray photoelectron spectroscopy (XPS).

From XPS elemental analysis of the bottom side (or ASNT side) of (A-T)<sub>10</sub>/PDMS, the Al/Si ratio could be determined and compared with pure ASNT film. The results are summarized in the Table 1 under.

**Table S1.** Comparison of Al/Si ratio.

Membrane	Al/Si ratio	Comment
Bottom side of (A-T) <sub>10</sub> /PDMS	0.05	Ti was also detected (See XPS spectra below)
Top side of (A-T) <sub>10</sub> /PDMS	—	No Al and Ti were detected
Pure ASNT film	1.3	Reference for comparison

It is worth mentioning that the approximate electron mean free path (depth of electron extraction) by X-ray is 2–10 nm, which is close to the thickness of ASNT network structure in (A-T)<sub>10</sub>/PDMS.

The smaller Al/Si ratio on the bottom side of (A-T)<sub>10</sub>/PDMS (Table S1) implies that the proportion of Si is higher than that of pure ASNTs. The additional Si should come from the interpenetrated PDMS into the ASNT network, signifying the embedment of PDMS into the ASNT-scaffold structure.

The XPS analysis was also conducted on the top (PDMS) side of the (A-T)<sub>10</sub>/PDMS nanomembrane for reference. The elemental analysis peaks are shown in Figure S2.

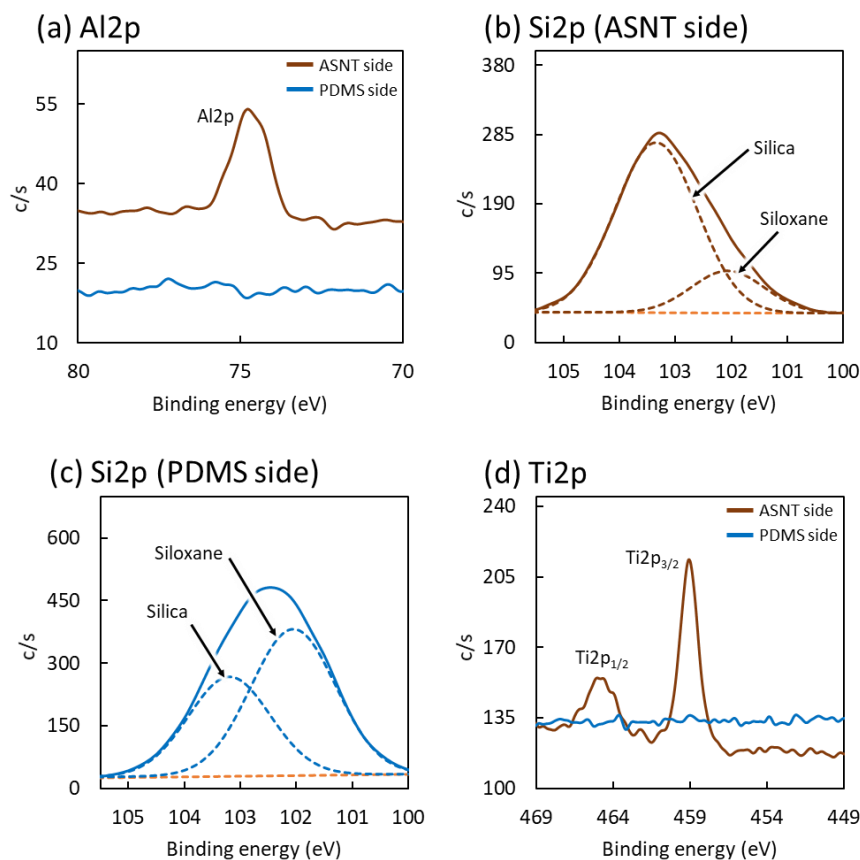


**Figure S2.** XPS elemental analysis. (a) Al is detected only on the ASNT side (bottom side). (b,c) Higher concentration of Si was observed, compared to pure ASNT. In addition, deconvolution of the Si2p peak obtained from the ASNT side indicated that there was siloxane form of Si ( $\sim 102.1$  eV). This confirms that portion of the PDMS reached the vicinity of the ASNT network side of (A-T)10/PDMS. However, the total amount of Si (on the ASNT side) is smaller than that of PDMS side—signifying that only small portion of PDMS could penetrate into the ASNT network structure. (d) Ti was detected only on the ASNT side of the membrane.

## 5. Investigation of mechanical properties

### 5.1. Bulging test

Mechanical properties of the nanomembranes were evaluated by bulging test,<sup>4–6</sup> a well-known technique to determine mechanical properties of supported and freely suspended nanomembranes. In this work, we employed hydraulic bulge test using distilled water as a source of mechanical pressure exerted on nanomembranes. Water was chosen because it has no swelling effect on PDMS.<sup>7</sup> Membranes were assembled as shown in Figure S3a.

The deflection of nanomembranes due to applied pressure (Figure S3c) was used to calculate stress, strain and biaxial modulus according to the following equations;<sup>4,5</sup>

$$\text{Stress, } \sigma = \frac{P(a^2+d^2)}{4td} \quad (1)$$

$$\text{Strain, } \varepsilon = \frac{S-S_0}{S_0} \quad (2)$$

$$\text{Biaxial modulus, } Y = \frac{3Pa^4}{8td^3} \quad (3)$$

where  $P$  is the applied pressure,  $a$  is the radius of active nanomembrane,  $t$  is nanomembrane thickness determined by SEM,  $d$  is deflection of the nanomembrane, and  $S$  and  $S_0$  are final and initial lengths of the curve in Figure S3c. When considering the effect of elastic constants on the accuracy of spherical membrane equations,<sup>4</sup> the actual biaxial modulus can be written simply as;

$$Y_{\text{act}} = \frac{Y_{\text{cal}}}{1-0.241\nu} \quad (4)$$

where  $\nu$  is the Poisson's ratio (a value of 0.3 is assumed in all calculations).

## 5.2. Control test

Stiffness of the tape used (thickness: 50  $\mu\text{m}$ , Teraoka Seisakusho Co., Ltd) was evaluated by a control test (Figure S2b). Water was loaded directly on the tape inside the tube and the possibility of deflection was checked. The tape was so stiff that it doesn't show any deflection up to 15 g water loading (which was the highest load added).

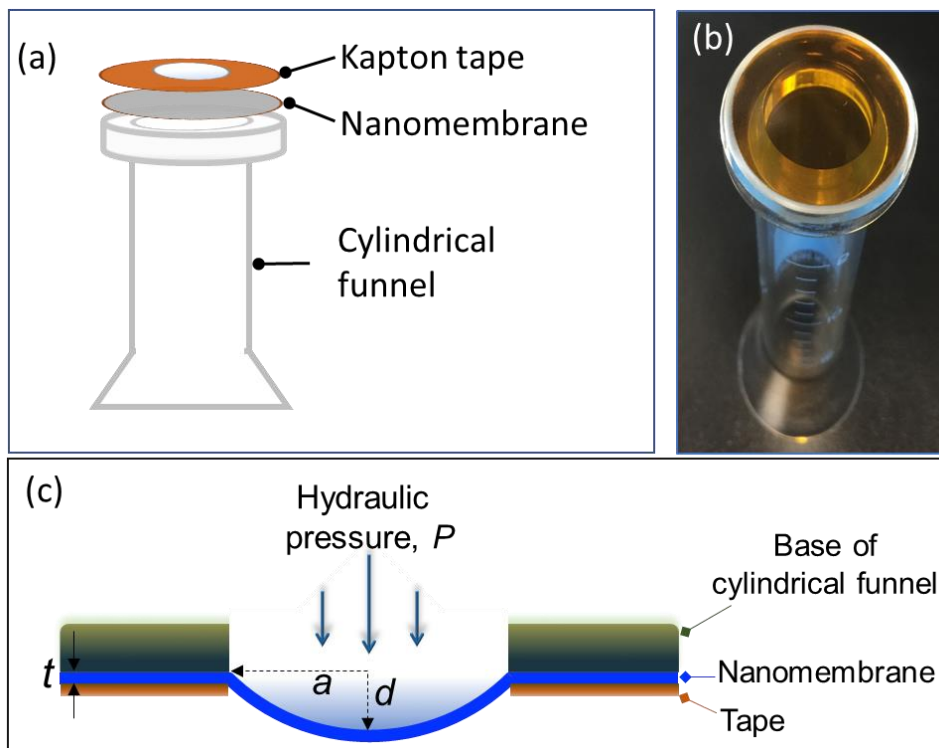


Figure S3. (a) Schematic illustration of membrane assembly for bulging test. (b) Cylindrical funnel in which one side was closed by a tape for control experiment. Water was loaded on the full-size tape without membrane. (c) Schematic description of mechanical property determination parameters;  $t$  = nanomembrane thickness,  $a$  = radius,  $d$  = deflection.

## Reference

- (1) Farmer, V. C. Synthetic Imogolite: Properties, Synthesis, and Possible Applications. *Clay Miner.* **1983**, 18 (4), 459–472.
- (2) Mersha, A.; Selyanchyn, R.; Fujikawa, S. Preparation of Large, Ultra-Flexible and Free-Standing Nanomembranes of Metal Oxide–polymer Composite and Their Gas Permeation Properties. *Clean Energy* **2017**, 1 (1), 1–10.
- (3) Johnston, I. D.; McCluskey, D. K.; Tan, C. K. L.; Tracey, M. C. Mechanical Characterization of Bulk Sylgard 184 for Microfluidics and Microengineering. *J. Micromechanics Microengineering* **2014**, 24 (3), 035017.
- (4) Small, M. K.; Nix, W. D. Analysis of the Accuracy of the Bulge Test in Determining the Mechanical Properties of Thin Films. *J. Mater. Res.* **2011**, 7, 1553–1563.

- (5) Kojio, K.; Nagano, C.; Fujimoto, A.; Nozaki, S.; Yokomachi, K.; Kamitani, K.; Watanabe, H.; Takahara, A. In Situ Synchrotron Radiation X-Ray Diffraction Studies on Molecular Aggregation Structure of Nylon 12 Films during Bulge Testing. *Soft Matter* **2018**, *14* (9), 1659–1664.
- (6) Schuster, C.; Rodler, A.; Tscheliessnig, R.; Jungbauer, A. Freely Suspended Perforated Polymer Nanomembranes for Protein Separations. *Sci. Rep.* **2018**, *8* (1), 1–11.
- (7) Lee, J. N.; Park, C.; Whitesides, G. M. Solvent Compatibility of Poly(Dimethylsiloxane)-Based Microfluidic Devices. *Anal. Chem.* **2003**, *75* (23), 6544–6554.